Jurnal Mesin Nusantara, Vol. 6, No. 1, Juni 2023, Hal. 24-34
e-ISSN : 2621-9506, p-ISSN : 2775-7390
DOI : 10.29407/jmn.v6i1.18233

Mechanical Properties of Welding API 5l X-65 Cladded UNS N08825 Material Due To The Effect of Welding Repair

Defi Pramesti [1)], Winarto[2)]

[1,2)] Department of Metallurgy and Material Engineering, Faculty of Engineering, Universitas Indonesia

E-mail: [1)] defi.pramesti@ui.ac.id [2)] winarto@metal.ui.ac.id

Abstract

This study evaluate the mechanical characteristics and microstructure of API 5L X-65-clad UNS N08825 during repair welding. Gas tungsten arc welding (GTAW) and shielded metal arc welding were used in combination to carry out the welding and the repair welding (SMAW). Filler metals ER NiCrMo3 and E NiCrMo3 were used throughout the GTAW and SMAW welding processes. The first specimen served as the primary focus, after which the weld areas of the remaining four specimens were ground, re-beveled, and then re-welded using the same parameters. It performed tensile testing, bending tests, Impact Charpy tests, macro photography tests, and Vickers hardness tests. Repairs weld carried out, the heat-affected zone's hardness in the capping region increased. The findings of the tensile test demonstrate that the tensile strength is not considerably impacted by the welding repair at any particular welding repair location. The biggest decline in the number is caused by the welding repair at PTR 2, which is 0.83 percent. The heat affected area (FL) value decreased by 10.44 percent according to the charpy impact test results. The PTR 1 and PTR 2 areas in the weld metal area had the lowest charpy impact test results, respectively, of 88 J and 258 J.

Keywords: Welding repair, Incoloy 825, API 5L X65, Mechanical properties, Destructive testing.

1. INTRODUCTION

As the pace of global industrialization quickens and energy demand rises, oil and gas exploration and production are progressively moving into deep-water and seabed locations. A highly corrosive environment is created by the presence of, hydrogen sulfide, chlorides and carbon dioxide in crude oil and natural gas that have just been taken from the seabed. Carbon steel pipes with an interior layer made of a corrosion-resistant alloy can be made to meet the toughest corrosion resistance, durability, and cost-effectiveness requirements to solve this problem. Clad pipes are 25–50% less expensive and use less corrosion-resistant alloy material than pipes made wholly of corrosion-resistant alloys [1].

Diterima 29 Juni 2022; direvisi terakhir 13 Juni 2023; diterbitkan 30 Juni 2023

Pipes constructed from steel grades with poor corrosion resistance Q235, 16Mo3, AISI 8630 steel, P235GH are widely coated with nickel-based superalloys (e.g. Inconel 625) as protective coatings. The study used X65 steel, a material frequently used in the transportation of oil and gas [2]. A structure with the necessary mechanical properties and corrosion resistance can be made by overlay welding the nickel-based alloy onto the X65 steel tubing. As a solid solution reinforced superalloy with good corrosion resistance, the nickel-based 625 alloy widely employed in the petroleum, chemical, aerospace, and other industrial sectors [3]. Potential engineer are searching for more tightly regulated financially alternatives to Nickel based corrosion-resistant alloys whenever possible in construction by using nickel-based 825 alloy due to the prohibitively expensive raw materials such as nickel and molybdenum and the resulting price volatility in superalloys [4].

Repair welding is an important maintenance and repair activity. The volume of repair and maintenance in the metal business is significantly greater than the volume of manufacture. The number of repairs is not limited in welding processes such as API-1104 [5] and ASME Section IX [6]. Fourth weld repairs are possible in the same spot seamless API X52 micro alloyed steel pipe when it was discovered that the effects of repeated repairs have been studied [7]. There has been relatively little research on the effects on mechanical properties and corrosion repair welding, and the majority of these studies are based on finite element simulation [8]. Due to the impact of welding repairs for pipelines, this issue is addressed in the current characterisation of welding API 5L X-65 cladded UNS N08825.

2. EXPERIMENT METHOD

a. Material and welding

API X-65 material pipe Cladded UNS N08825 with outside dimensions of 508 mm, 400 mm, and 23 mm was manufactured and welded using electrode E NiCrMo3 with a 3.2 mm diameter and filler metal ER NiCrMo3 with a 2.4 mm diameter, respectively.

A single V-joint with a bevel angle of 30, a root face of 1, and a spacing of 3 mm underwent welding. The welding operation was carried out in fixed horizontal for the root until the hot pass using straight polarity and gas tungsten arc welding, and for the hot pass until the capping using shielded metal arc welding with straight polarity and direct current. Using argon gas that is 99.998% pure and flowing at a rate of 15L/min, respectively, for both purging and shielding. After achieving 50% weld thickness, the external clamp used during the welding operation was removed. Shielding gas is purged using a mechanism when an oxygen analyzer detects up to 50 ppm of it.

This study used welding to examine how the iterative repair procedure affected the development of the corrosion resistance and mechanical qualities of API 5L X-65 Cladded UNS N08825. Both shielded metal arc welding (SMAW) and gas tungsten arc welding (GTAW) techniques were used to join five samples.

Table 1. Identification for sample

No	No Sample	Dimension	Identification
1	RI-13	Ø 508 x 400 x 23 mm	Main (M)
2	RI-14	Ø 508 x 400 x 23 mm	Capping Partial Repair (CPR)
3	RI-15	Ø 508 x 400 x 23 mm	Partial Thickness Repair (PTR 1)
4	RI-16	Ø 508 x 400 x 23 mm	Partial Thickness Repair (PTR 2)
5	RI-17	Ø 508 x 400 x 23 mm	Through Thickness Repair (TTR)

The first sample was prepared as an original weld, then the weld area was excavated with a grinder, and re-prepared in the same area which was then re-welded.

Table 2. Welding repair sequences

No	No Sample	Identification	Excavation by grinding	Joint Configuration
1	RI-13	Main (M)	-	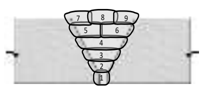
2	RI-14	Capping Partial Repair (CPR)	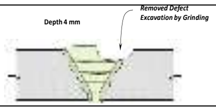	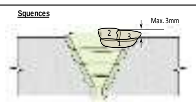
3	RI-15	Partial Thickness Repair (PTR 1)	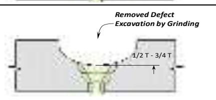	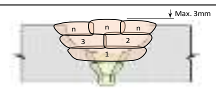
4	RI-16	Partial Thickness Repair (PTR 2)	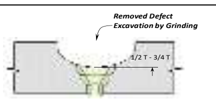	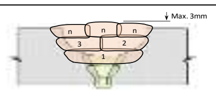
5	RI-17	Through Thickness Repair (TTR)	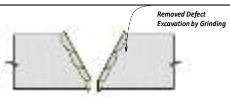	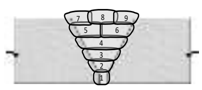

b. Destructive testing

These samples were then tested to study the corrosion resistance and mechanical properties of the welds. Destructive tests carried out in this study were tensile test to determine the strength of the weld. Tensile test conducted in accordance with API 1104. According to API 1104 bending test conducted use transverse specimen, it carried out to determine pore or crack defects in the weld metal. Impact test to determine the toughness of the weld due to heat input in the weld metal, fusion line (HAZ) and base metal (FL+2), it conducted in accordance with ASTM E23-18. According to API 1104 nick break test conducted. Hardness vickers test to determine the hardness value in the weld area according to ASTM E92-17. The value of the results of the mechanical test will be compared on each test specimen so that it can be seen the effect of welding repair on the specimen. Macro examination is carried out to display macro photograph of the weld area, this can see the weld if there are parts that are not fused.

3. RESULT AND DISCUSSION

a. Macro photos

Macro photos of main welds, CPR, PTR 1, PTR 2, and TTR are shown in Figure 4. xx. it is clear that the three zones are different, namely base metal (BM), heat affected zone (HAZ)and weld metal (WM). From the overall results of macro photos, it is not seen that there are welding defects that occur in all welding repair processes. This is because at the time of welding, strict control parameters have been carried out against the possibility of external contaminants that can be the source of the formation of welding defects. The controls include preheating before welding, monitoring the oxygen content below 50 ppm and measuring using an oxygen analyzer, using a grinding stone that is free of iron, in addition, the welding process is carried out using a shield & shielding against argon ultra gas. high purity (UHP)with a purity of 99.998% to protect the root protected during the welding process. From the macro photo in Figure 4.xx it can also be seen that the API 5L X65 cladded UNS08825 welding results have a uniform HAZ area in all welding repair processes, which is about 1.5 – 2 mm using manual measurements.

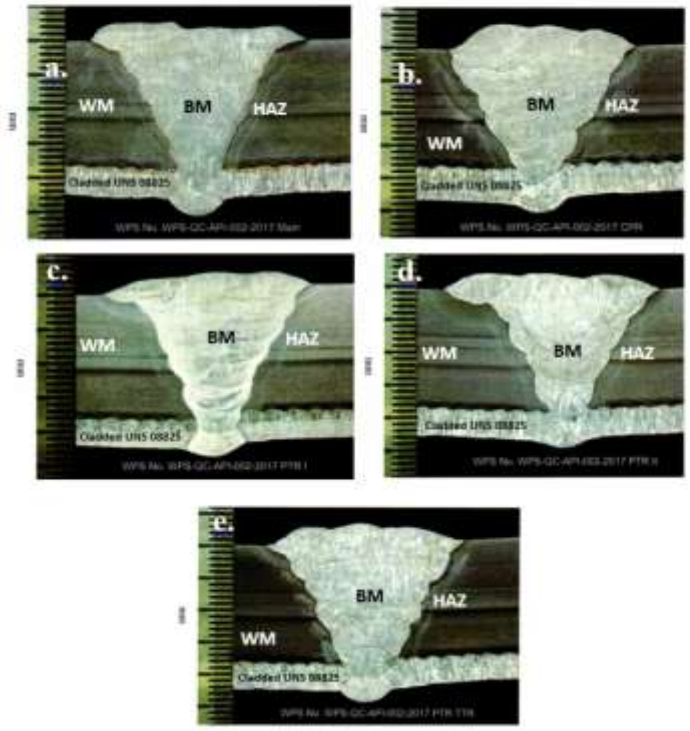

Figure 1. Microstructure a) Main, b) CPR, c) PTR 1, d) PTR 2 dan e) TTR

b. Microstructure

In this study, a photo of the microstructure was taken with a magnification of 500x resulting in a photo of the microstructure of the base metal in Figure 4.xx below. This base material has an irregular phase structure and polygonal ferrite, ferrite carbide aggregate (FC), ferrite with aligned second phase (FS(A)) and ferrite with non-aligned second phase (FS(NA)). The image also shows a fine A-M distribution (retained austenite+martensite) which characterizes the microstructure of the mixture.

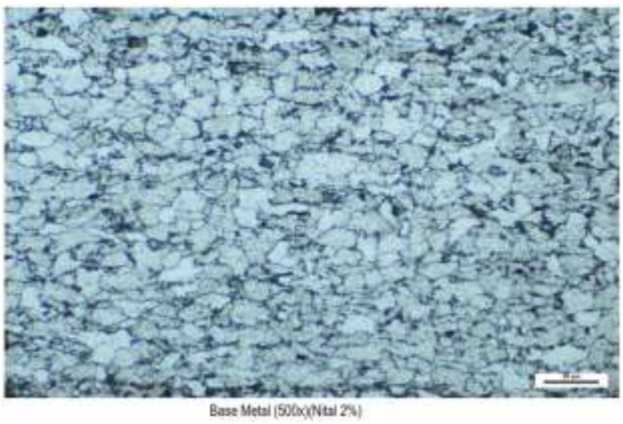

Figure 2. Microstructure at base metal API 5L X65

Figure 2. shows the microstructure in areas with different locations for the welding repair process, namely Main, CPR, PTR 1, PTR 2 and TTR, while Figure 4.3 shows the microstructure of weld metal (WM) on the cap. The observation of differences in microstructure shows that there are differences in the material on the base metal and weld metal because it uses the same welding wire as the UNS 08825 cladded material.

The HAZ area in the Main welding process shows a rounded grain shape compared to the HAZ area in the CPR, PTR 1 and TTR welding repair processes. In the repair process of PTR 2 welding the grain shape experienced rounding compared to PTR 1. This was due to the influence of heat given to the material so that it experienced a grain enlargement process compared to the previous PTR 1 welding repair process. The microstructure in the weld metal area which has a dendritic shape because it is nickel-based, can be seen in Figure 4 a) the microstructure in the capping area of the main welding process has a smooth dendritic shape. In Figure 4 b) after performing CPR, dendritic enlargement occurs due to the effect of the repair process carried out by capping. Likewise, in the repair process for welding PTR 1 and PTR 2, the same dendritic forms as in the CPR process, but different from the repair process for TTR welding, because during the welding process there is a heating effect on the layer so that the shape of the dendritic grains enlarges and is more round in shape. Furthermore, on observing the microstructure using an optical microscope, no indication of the formation of MC carbides such as M6C or M23C6 was found.

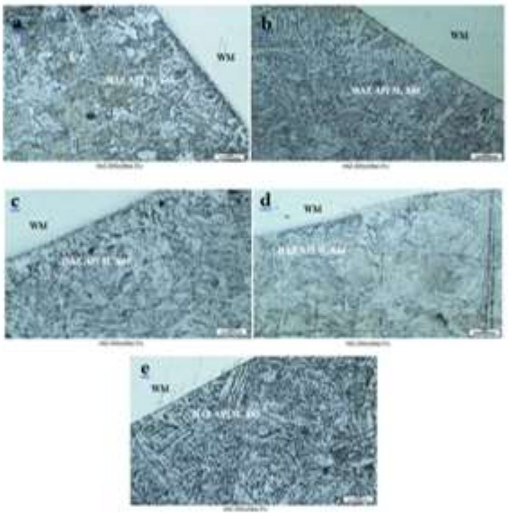

Figure 3. Microstructure of base metal API 5L X65 at location HAZ a) Main b) CPR c) PTR 1 d) PTR 2 e) TTR

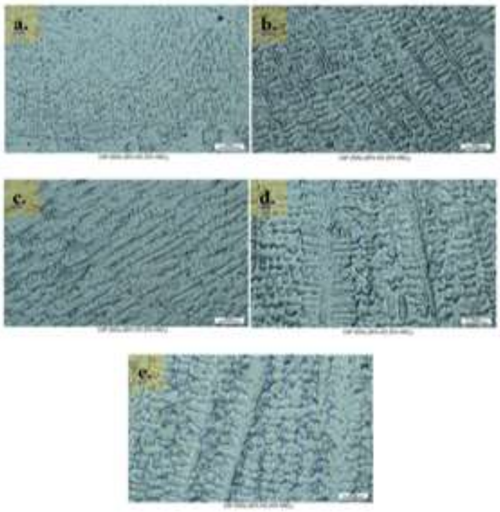

Figure 4. Microstructure of weld metal on capping a) Main b) CPR c) PTR 1 d) PTR 2 e) TTR

c. Tensile Test

In the initial welding process (Main) it is processed using the parameters in table 4.1 and produces a tensile strength value of 583 N/mm2, this tensile test value is still included in the minimum acceptability standard that must be achieved according to API 5L, which is a minimum of 535 N/mm2. The tensile test value in the repair welding process produces a maximum value of strength in the CPR repair welding process which reaches 591 N/mm2 and produces a minimum strength value in the PTR 2 welding repair process, which is 578 N/mm2 below the value of the M welding process.

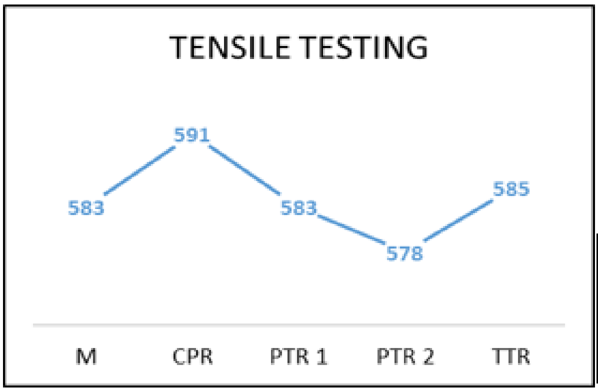

No	No Sample	Identification	Tensile (N/mm^2)	Lokasi Patah	Tipe patahan
1	RI-13	M	583	Logam induk	Ulet
2	RI-14	CPR	591	Logam induk	Ulet
3	RI-15	PTR 1	583	Logam induk	Ulet
4	RI-16	PTR 2	578	Logam induk	Ulet
5	RI-17	TTR	585	Logam induk	Ulet

Figure 5 The average tensile testing result

d. Charpy Impact Test

The charpy impact testing process is carried out to see the value of the toughness of the material on the welding repair process variable. The impact testing process is carried out in 3 areas, namely weld metal (WCL), HAZ (FL) and base metal (FL+2) according to ASTM E23-18 standards. Figure 5 shows the results of the charpy impact toughness test of each welding repair process variable and the overall impact value is included in the acceptance criteria according to the API 1104 standard. The charpy impact test result in the WCL area produces the smallest value compared to the FL & FL+ area. 2. The highest charpy impact value was found in the base metal area (FL+2). In the base metal (FL+2) and HAZ (FL) areas after the welding repair process is carried out in Figure 6. the graph shows a downward trend, in contrast to the Weld metal (WCL) area, there is an upward trend in the value of the charpy impact test.

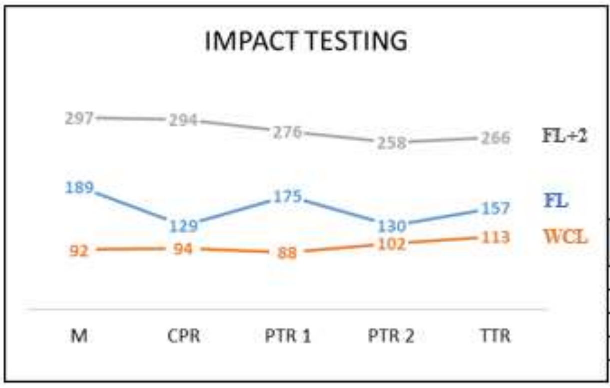

No	No Sample	Identification	Impact (J)		
			WCL	FL	FL+2
1	RI-13	M	92	189	297
2	RI-14	CPR	94	129	294
3	RI-15	PTR 1	88	175	276
4	RI-16	PTR 2	102	130	258
5	RI-17	TTR	113	157	266

Figure 6. Impact testing result

e. Hardness Test

The results of the hardness test show that the average value of the Vickers HV 10 microhardness test with a load of 10 kg can be seen in Figure 6. In general, the average hardness value obtained from each repair welding process at a particular location does not show a significant difference. on the hardness value of the parent metal, and it can be seen in the graph that the trend of the hardness value decreases slightly after the welding repair process is carried out. The hardness value obtained also shows that the weld metal (WM) area has the highest value compared to the HAZ area and the parent metal. In the HAZ area, the hardness value decreased compared to the base metal area, although it was not significant. This increase in the hardness of the weld metal can be caused by the welding wire used is nickel-based which has a higher hardness value than the hardness value of the parent metal which is made of carbon steel.

Lokasi	Titik pengujian	Rata-rata nilai kekerasan (HV)				
		Main	CPR	PTR1	PTR2	TTR
BM	1	206	210	197	204	208
	2	199	212	198	198	208
	3	200	210	199	198	210
HAZ	4	200	204	199	194	205
	5	206	204	198	195	205
	6	206	202	202	194	203
WM	7	241	227	228	225	234
	8	241	225	230	227	247
	9	243	231	222	227	240
HAZ	10	201	193	194	194	197
	11	199	194	188	193	198
	12	194	193	185	191	191
BM	13	204	197	201	200	206
	14	201	199	200	197	202
	15	202	197	197	196	198

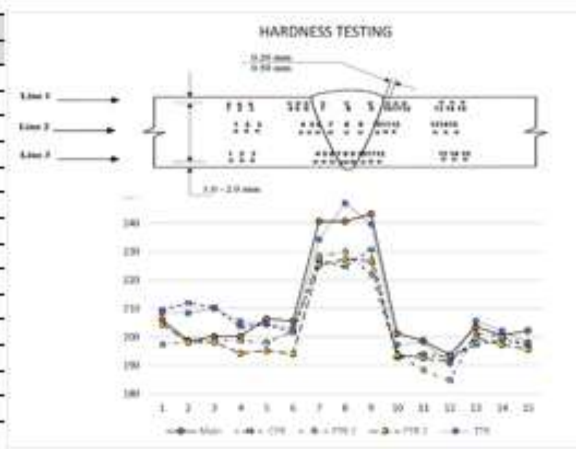

Figure 7. Comparison average distribution of hardness

From the results of the overall hardness values that exist individually or the average obtained is still included in the acceptance criteria in the industrial world which refers to API 1104, where the average hardness value is limited to a maximum of 280 HV. The relatively small decrease in hardness in HAZ at PTR 2 occurs because the heating cycle gives the effect of more heat input to the material, resulting in grain enlargement in the weld results. The hardness value which is most visible decreases is in the HAZ area, where the HAZ area of the main welding process has a higher average hardness value than in the welding repair process. This is because the welding repair process has accumulated more heat input than the Main welding process. In Figure 7. c) the results in the capping area show the highest and regular hardness values because the measurement of hardness will be influenced by the influence of heat received by the material, in the weld metal area not all parts have changed, meaning that the welding repair process is based on the repair location, then the capping area will be more precise in getting the hardness value that is affected by the welding repair process. Figure 7. a) produces a graph that has the highest hardness value because the hardness test is taken in the Root area where the root is cladded UNS 08825 which has a nickel base material which has a higher value than the middle part of the weld metal and the root is taken for hardness in the lower part. API 5L X65 base material.

4. CONCLUSION

Based on the results of research on the characterization of API 5L X-65 Cladded UNS N08825 material due to the effect of welding repair, conclusions can be drawn including:

1) The tensile test results show that the welding repair process does not significantly affect the tensile strength value at all welding repair locations. The biggest decrease value, which is 0.83%, occurred in the welding repair process at PTR 2 location.
2) The results of the charpy impact test show a decrease in the value of the heat affected area (FL) by 10.44%. The lowest charpy impact test results in the weld metal area occurred at PTR 1, which was 88 J and in PTR 2 area, which was 258 J. The impact test results in the base metal area (WCL) had the lowest average value compared to the other two areas. FL and FL+2 is 97.8 J.
3) The results of the hardness test show that the weld metal (WM) has the highest average value, which is 233 HV.
4) The results of the observation of the microstructure using an optical microscope in the TTR welding repair process in the HAZ area experienced coarsening of the grain shape and elongated shape, while in the weld metal (WM) area the shape changed to a more rounded shape and enlarged in the TTR repair process.

5. ACKNOWLEDGMENTS

The author thanked the Directorate of Research and Community Services of the University of Indonesia and the Counsellor.

6. REFERENCES

[1] N. Sayyar, M. Shamanian, B. Niroumand, J. Kangazian, EBSD observations of microstructural features and mechanical assessment of Incoloy 825 alloy/ AISI 321 stainless steel dissimilar welds, Manufacturing Processes. 60 (2020) 86-95.

[2] L. Xu, J. Zhang, Y. Han, L. Zhao, H. Jing, Insigh into the intergranular corrosion of overlay welded joints of X65-Inconel 625 clad pipe and its relationship to damage penetration, Corrosion Science. 160 (2019).

[3] K. He, L. Dong, Q. Wang, H. Zhang, Y. Li, L. Liu, Z. Zhang, Comparison on the microstructure and corrosion behavior of Inconel 625 cladding deposited by tungsten inert gas and cold metal transfer process, Surface and Coating Technology. 435 (2022).

[4] J. kangazian, M. Shamanian, Microstructure and mechanical characterization of Incoloy 825 Ni-based alloy welded to 2507 super duplex stainless steel through dissimilar friction stir welding, ScienceDirect. 29 (2019) 1677-1688.
[5] API STANDARD 1104: Welding of pipeline and related facilities. 20 ed.; 2005.
[6] ASME SECTION IX: Qualification standard for welding and brazing procedures, welders, brazers, and welding and brazing operators; 2002.
[7] O.E. Vega, J.M. Hallen, A. Villagomez, A. Contreras, Effect of multiple repairs in girth welds of pipelines on the mechanical properties, Material Characterization. 59 (2008) 1498-1507.
[8] C. P. Alvares, J. C. F Jorge, L. F.G de Souza, L. S. Araujo, M. C. Mendes, H. N. Ferneze, Microstructure and corrosion properties of single layer Inconel 625 weld cladding obtained by the electroslag welding process, Materials Research and Technology. 9 (2020).